

## Relationship between boundary misorientation angle and true strain during high temperature deformation of 7050 aluminum alloy

HU Hui-e(胡会娥)<sup>1</sup>, YANG Li(杨 丽)<sup>1</sup>, ZHEN Liang(甄 良)<sup>1</sup>,  
SHAO Wen-zhu(邵文柱)<sup>1</sup>, ZHANG Bao-you(张宝友)<sup>1</sup>

School of Materials Science and Engineering, Harbin Institute of Technology, Harbin 150001, China

Received 17 October 2007; accepted 4 April 2008

**Abstract:** Tensile tests of solid solution treated 7050 aluminum alloy were conducted to different strain degrees (0.1, 0.4, 0.6 and failure) at 460 °C with the strain rate of  $1.0 \times 10^{-4}$ – $1.0 \times 10^{-1} \text{ s}^{-1}$ . The boundary misorientation angle evolution during hot deformation of the 7050 aluminum alloy was studied by EBSD technique and the fracture surfaces were observed using SEM. A linear relationship between the increase in the average boundary misorientation angle and the true strain at different strain rates is assumed when aluminum alloy is deformed at 460 °C. The increasing rate of average boundary misorientation angle is 15.1°, 15.7° and –0.75° corresponding to the strain rate of  $1.0 \times 10^{-4}$ ,  $1.0 \times 10^{-2}$  and  $0.1 \text{ s}^{-1}$ , respectively. The main softening mechanism is continuous dynamic recrystallization when the strain rates are  $1.0 \times 10^{-4}$  and  $1.0 \times 10^{-2} \text{ s}^{-1}$ , and it is dynamic recovery when strain rate is  $0.1 \text{ s}^{-1}$ .

**Key words:** boundary misorientation angle; aluminum alloy; electron backscatter diffraction(EBSD); high temperature deformation; microstructure

### 1 Introduction

High-strength aluminum alloys have been widely used for aeronautical applications due to their desirable mechanical properties[1–4], which are greatly influenced by the microstructure characteristics of these alloys. Boundary misorientation angle is a typical microstructure parameter that affects the ultimate property of high-strength aluminum alloy with high stacking fault energy. However, it has not been studied in detail because of the obstacles of traditional analysis techniques[5]. Recently, the electron backscatter diffraction(EBSD) technique has been widely used to solve this problem. Some studies on boundary misorientation angle using EBSD have been reported[6–13].

There have been some researches about the boundary misorientation angle evolution during high temperature deformation of aluminum alloy[5, 14–16]. LIU et al[5] suggested that the average boundary misorientation angle is strongly dependent on the strain during high temperature deformation of Al-Li alloy and the strain to which the average boundary misorientation angle reaches about 20° increases with increasing strain

rate. The superplastic flow of Al-Li alloy was studied by XUN et al[14], and a linear relationship between the increase in the average boundary misorientation angle and cumulative tensile strain in the early stages of superplastic flow was assumed. There is no common conclusion about the change of boundary misorientation angle during high temperature deformation of aluminum alloy. To the best of our knowledge, there are a few researches reported on the effect of strain rate on the boundary misorientation angle evolution during high temperature deformation. So it is necessary to acquire the data on the issue to understand the boundary misorientation angle evolution during high temperature deformation of aluminum alloy.

In this work, the boundary misorientation angle evolution of 7050 aluminum alloy during high temperature deformation with different strain rates was studied. The main aim is to acquire the relationship between the average angle and true strain with different strain rates.

### 2 Experimental

The rolled plate of 7050 aluminum alloy used in the present work was provided by Beijing Institute of

Aeronautical Materials, China, with 80 mm in thickness and T7451 temper. The compositions were Al-(5.7–6.7)Zn-(1.9–2.6)Mg-(2.0–2.6)Cu-0.1Zr-0.15Fe-0.12Si-0.10 Mn (mass fraction, %). Tensile specimens with 5 mm gage width and 20 mm gage length were machined with the tensile axis parallel to the rolling direction. The tensile specimens were solid solution treated at 477 for 1 h, and then quenched into water. Tensile tests were conducted on Instron 5500R at 460 with the strain rate of  $1.0 \times 10^{-4}$ ,  $1.0 \times 10^{-2}$  and  $0.1 \text{ s}^{-1}$ , respectively. In order to study the boundary misorientation angle evolution of the 7050 aluminum alloy during high temperature deformation, the tensile tests were interrupted and the specimens were unloaded after being deformed to predetermined true strains ( $\varepsilon=0.1$ ,  $\varepsilon=0.4$ ,  $\varepsilon=0.6$  and failure). The samples for EBSD measurement were mechanically polished followed by electro polishing using 10%  $\text{HClO}_4$  (volume fraction) acids in alcohol at  $-30$  and a voltage of 30 V[17] to remove the deformation layer. The samples were examined and analyzed using HKL Channel 5 software in a JEOL 733 electron probe at a sample tilt of  $70^\circ$ , with an accelerating voltage of 20 kV. Step size of the maps was 1  $\mu\text{m}$ . The EBSD analysis was conducted on the RD(rolling direction)–ND(normal direction) surface of the plate. Fracture surface of tested specimen was analyzed by a Hitachi S-4700 scanning electron microscope(SEM).

### 3 Results and discussion

The maximum true strains of the 7050 aluminum alloy deformed at strain rates of  $1.0 \times 10^{-4}$ ,  $1.0 \times 10^{-2}$  and  $0.1 \text{ s}^{-1}$  are 1.14, 1.32 and 1.09, respectively. Fig.1 shows grain boundary maps near fracture surfaces of 7050 aluminum alloy deformed at 460 with different strain rates. In the grain boundary maps, coarse black lines are high angle grain boundaries ( $> 15^\circ$ ) and fine black lines are low angle grain boundaries ( $2^\circ\text{--}15^\circ$ ). It is shown that the size and shape of the grains in the 7050 aluminum alloy tested under different deformation conditions are different. The microstructure is characterized by large size and elongated grains and some fine equiaxed grains along the big angle boundaries when the strain rate is  $0.1 \text{ s}^{-1}$ . Some low angle grain boundaries are observed in the large size and elongated grains (see Fig.1(c)). The grain boundary maps of the 7050 aluminum alloy deformed at  $1.0 \times 10^{-4}$  and  $1.0 \times 10^{-2} \text{ s}^{-1}$  consist of only small equiaxed grains, and a small quantity of low angle boundaries are observed (see Figs.1(a) and (b)).

The relative frequencies of low angle grain boundaries ( $2^\circ\text{--}15^\circ$ ) when the specimens were deformed at different strain rates ( $1.0 \times 10^{-4}$ ,  $1.0 \times 10^{-2}$  and  $0.1 \text{ s}^{-1}$ )

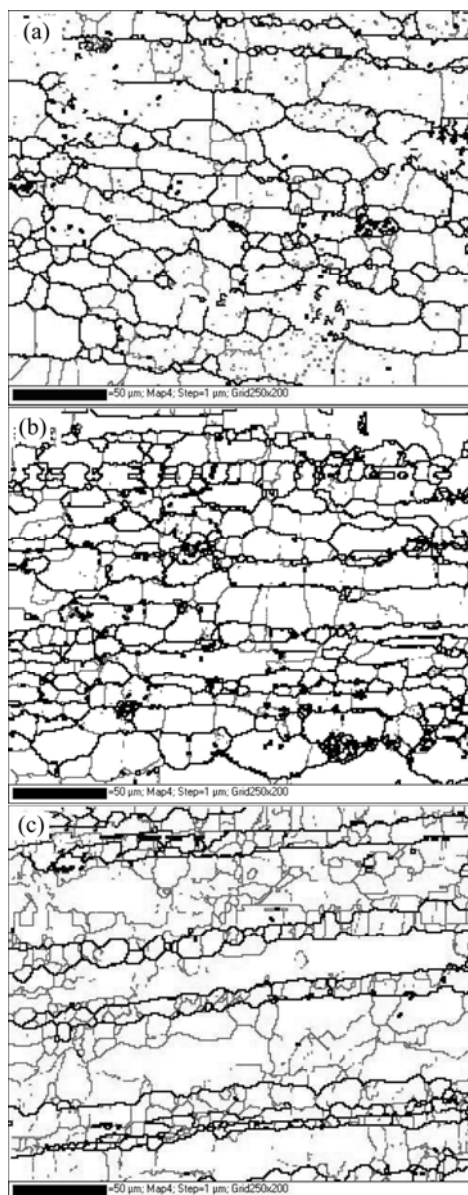


**Fig.1** Grain boundary maps near fracture surface of 7050 aluminum alloy tested at 460 with different strain rates: (a)  $1 \times 10^{-4} \text{ s}^{-1}$ ; (b)  $1 \times 10^{-2} \text{ s}^{-1}$ ; (c)  $0.1 \text{ s}^{-1}$

to different true strains ( $\varepsilon=0.1$ ,  $\varepsilon=0.4$ ,  $\varepsilon=0.6$  and failure) are shown in Fig.2. It can be seen that the relative frequency of low angle grain boundaries decreases with the increase of true strain at strain rates of  $1.0 \times 10^{-4}$  and  $1.0 \times 10^{-2} \text{ s}^{-1}$ . When the strain rate is  $0.1 \text{ s}^{-1}$ , the relative frequencies of low angle grain boundaries are fluctuant with increasing true strain. Fig.2 suggests that the deformation behavior with the strain rate of  $0.1 \text{ s}^{-1}$  is different from that with the strain rate of  $1.0 \times 10^{-4}$  and  $1.0 \times 10^{-2} \text{ s}^{-1}$ .

Fig.3 shows the average boundary misorientation angles of the specimens deformed at different strain rates to different true strains. A linear relationship between the increases of the average boundary misorientation angle

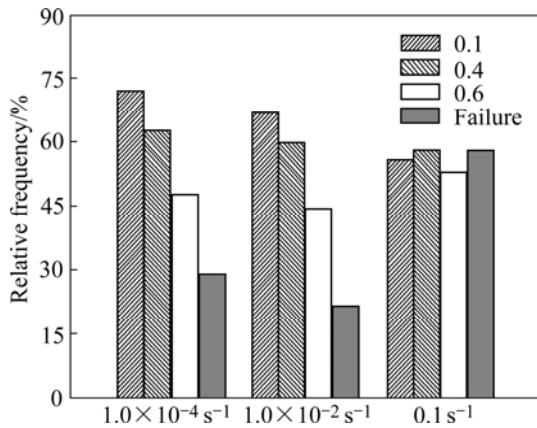


**Fig.2** Relative frequency of low angle grain boundaries (2°–15°) of samples deformed at different true strains

and the true strain at different strain rates can be assumed from the figure, which can be expressed as  $\Delta\theta=k\Delta\varepsilon$ , where  $\Delta\theta$  is the increase of the average boundary misorientation angle and  $\Delta\varepsilon$  is the increase of the true strain. The  $k$  value can be fixed by the slope of the straight fitting line in the plot of  $\Delta\theta$  against  $\Delta\varepsilon$ , which is 15.1°, 15.7° and -0.75° corresponding to the strain rate of  $1.0 \times 10^{-4}$ ,  $1.0 \times 10^{-2}$  and  $0.1 \text{ s}^{-1}$ , respectively. The difference of  $k$  value may result from different deformation mechanisms of the 7050 aluminum alloy deformed at 460 with different strain rates.

In the EBSD analysis, the boundary is defined as grain boundary when the boundary misorientation angle is higher than 15° and a low angle grain boundary is identified if the neighbor boundary misorientation angle exceeds 2°. The grain is classified as being deformed if the average boundary misorientation angle in a grain exceeds 2°. Some grains include in low angle grain boundaries, but whose internal boundary misorientation angle is below 2°. In that case the grain is classed as substructure. All the remaining grains are classified as

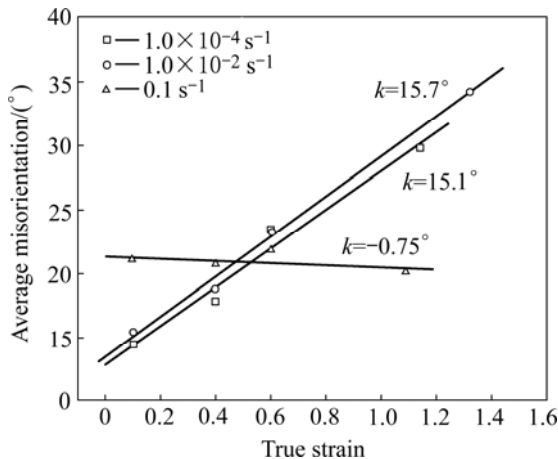


**Fig.3** Average boundary misorientation angles as function of true strain in 7050 aluminum alloy during high temperature deformation at 460 with different strain rates

being recrystallized. The relative volume fractions of three kinds of microstructures during high temperature deformation of the 7050 aluminum alloy are shown in Fig.4. It is shown that the relative volume fraction of the deformed grain is low during high temperature deformation at all strain rates. Substructural grains transform gradually to recrystallized grains with increasing strain when the strain rates are  $1.0 \times 10^{-2}$  and  $1.0 \times 10^{-4} \text{ s}^{-1}$ . The maximum relative fraction values of recrystallized grains are both larger than 75%, suggesting that the primary softening mechanism is dynamic recrystallization at these two strain rates. However, the relative volume fraction of recrystallized grains fluctuates with increasing strain at the strain rate of  $0.1 \text{ s}^{-1}$ , and the maximum volume fraction of recrystallized grains is 45%. The microstructure results show that the main softening mechanism is not dynamic recrystallization when the 7050 aluminum alloy is deformed at  $0.1 \text{ s}^{-1}$ , but it is dynamic recovery. So the less variations of average boundary misorientation angle of the 7050 aluminum alloy during high temperature deformation at  $0.1 \text{ s}^{-1}$  show that the main softening mechanism under the deformation condition is not dynamic recrystallization but dynamic recovery. The continuous increases of the average boundary misorientation angle during high temperature deformation at the strain rates of  $1.0 \times 10^{-4}$  and  $1.0 \times 10^{-2} \text{ s}^{-1}$  show that the main softening mechanism under the deformation conditions is continuous dynamic recrystallization. LIU et al[5] reported that the  $k$  value is about 17° in Al-Li alloy. Besides, the  $k$  value of 18.1° in Al-Li alloy was reported by XUN et al[14]. The different materials with different initial microstructures and different deformation conditions may be the primary causes of the variation of the  $k$  values.

Fig.5 shows the fracture surfaces of the 7050 aluminum alloy tested at 460 with different strain rates. The fracture surfaces of the 7050 aluminum

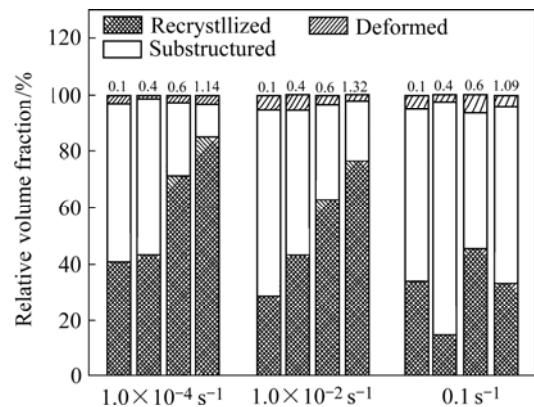


**Fig.4** Relative volume fraction of different microstructures of 7050 aluminum alloy deformed under different deformation conditions

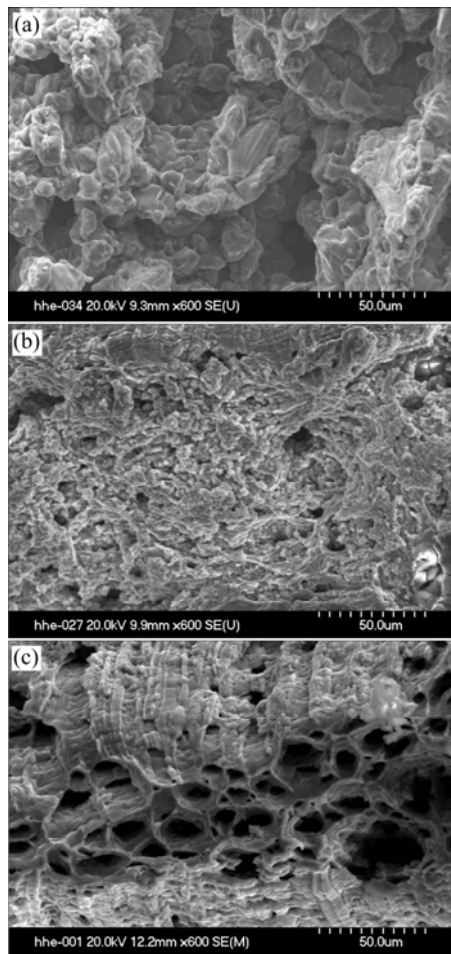


**Fig.5** SEM micrographs showing fracture surface of 7050 aluminum alloy tested at 460 °C with different strain rates: (a)  $1 \times 10^{-4} \text{ s}^{-1}$ ; (b)  $1 \times 10^{-2} \text{ s}^{-1}$ ; (c)  $0.1 \text{ s}^{-1}$

alloys, which are deformed at 460 °C with strain rates of  $1.0 \times 10^{-4}$  and  $1.0 \times 10^{-2} \text{ s}^{-1}$ , are ductile intergranular fracture characterized by relatively smooth surfaces, revealing the initial grain structure (see Figs.5(a) and (b)). These small size grains confirm that dynamic recrystallization is the main softening mechanism of the 7050 aluminum alloy deformed at 460 °C with the strain rate of  $1.0 \times 10^{-4}$  and  $1.0 \times 10^{-2} \text{ s}^{-1}$ . However, the fracture surface possesses the characteristics of ductile transgranular fracture characterized by dimples with different sizes and ductile intergranular fracture when the strain rate is  $0.1 \text{ s}^{-1}$  (see Fig.5(c)). The dimples in Fig.5(c) show that dynamic recrystallization is not the main softening mechanism. Otherwise, the results of fracture surfaces are in accordance with that of grain boundary maps.

## 4 Conclusions

1) The increase of average boundary misorientation angle of the 7050 aluminum alloy is proportional to the increase of the true strain during high temperature deformation at 460 °C and different strain rates ( $1.0 \times$

$10^{-4}$ ,  $1.0 \times 10^{-2}$  and  $0.1 \text{ s}^{-1}$ ).

2) The  $k$  values, the increasing rate of average boundary misorientation angle, are  $15.1^\circ$ ,  $15.7^\circ$  and  $-0.75^\circ$  corresponding to the strain rates of  $1.0 \times 10^{-4}$ ,  $1.0 \times 10^{-2}$  and  $0.1 \text{ s}^{-1}$ , respectively.

3) The main softening mechanism is continuous dynamic recrystallization when the strain rates are  $1.0 \times 10^{-4}$  and  $1.0 \times 10^{-2} \text{ s}^{-1}$ . However, dynamic recovery is the main softening mechanism when the 7050 aluminum alloy is deformed at  $0.1 \text{ s}^{-1}$ .

## References

- [1] WILLIAMS J C, STARKE E A. Progress in structural materials for aerospace systems [J]. *Acta Mater*, 2003, 51(19): 5775–5799.
- [2] WLOKA J, HACK T, VIRTANEN S. Influence of temper and surface condition on the exfoliation behaviour of high strength Al-Zn-Mg-Cu alloys [J]. *Corros Sci*, 2007, 49(3): 1437–1449.
- [3] ESCHAMPS A D, BRÉCHET Y. Influence of quench and heating rates on the ageing response of an Al-Zn-Mg-(Zr) alloy [J]. *Mater Sci Eng A*, 1998, 251(1/2): 200–207.
- [4] STILLER K, WARREN P J, HANSEN V. Investigation of precipitation in an Al-Zn-Mg alloy after two-step ageing treatment at 100° and 150 °C [J]. *Mater Sci Eng A*, 1999, 270: 55–63.
- [5] LIU Q, HUANG X X, YAO M. On deformation-induced continuous recrystallization in a superplastic Al-Li-Cu-Mg-Zr alloy [J]. *Acta Metall Mater*, 1992, 40(7): 1753–1762.
- [6] EGHBALI B, ABDOLLAH-ZADEH A, BELADI H, HODGSON P D. Characterization on ferrite microstructure evolution during large strain warm torsion testing of plain low carbon steel [J]. *Mater Sci Eng A*, 2006, 435/436: 499–503.
- [7] EDDAHBI M, CARRE F, RUANO O A. Deformation behavior of an Al-Cu-Mg-Ti alloy obtained by spray forming and extrusion [J]. *Mater Lett*, 2006, 60(27): 3232–3237.
- [8] WAHABI M E, GAVARD L, CABRERA J M, PRADO J M, MONTHEILLET F. EBSD study of purity effects during hot working in austenitic stainless steels [J]. *Mater Sci Eng A*, 2005, 393(1/2): 83–90.
- [9] XUN Y, TAN J. EBSD characterization of 8090 Al-Li alloy during dynamic and static recrystallization [J]. *Mater Charact*, 2004, 52(3): 87–193.
- [10] GROEBER M A, HALEY B K, UCHIC M D, DIMIDUK D M, GHOSH S. 3D reconstruction and characterization of polycrystalline microstructures using a FIB-SEM system [J]. *Mater Charact*, 2006, 57(4/5): 259–273.
- [11] DU Y X, ZHANG X M, YE L Y, LUO Z H. Recrystallization behavior of high purity aluminum at 300 °C [J]. *Trans Nonferrous Met Soc China*, 2006, 16(6): 1307–1312.
- [12] HU H E, ZHEN L, ZHANG B Y, YANG L, CHEN J Z. Microstructure characterization of 7050 aluminum alloy during dynamic recrystallization and dynamic recovery [J]. *Mater Charact*, 2008, 10.1016/j.matchar. 2007. 09. 010.
- [13] HU H E, ZHEN L, ZHANG B Y, YANG L, CHEN J Z. Microstructure evolution in hot deformation of 7050 aluminum alloy with coarse elongated grains [J]. *Mater Sci Technol*, 2008, 24(3): 281–286.
- [14] XUN Y, TAN M J, NIEH T G. Grain boundary characterization in superplastic deformation of Al-Li alloy using electron backscatter diffraction [J]. *Mater Sci Technol*, 2004, 20: 173–180.
- [15] TSUZAKI K, MATSUYAMA H, NAGAO M. High-strain rate superplasticity and role of dynamic recrystallization in a superplastic duplex stainless steel [J]. *Mater Trans JIM*, 1990, 31: 983–994.
- [16] LIU J, CHAKRABARTI. Grain structure and microtexture evolution during superplastic forming of a high strength Al-Zn-Mg-Cu alloy [J]. *Acta Mater*, 1996, 44(12): 4647–4661.
- [17] CAO W Q, GODFREY A, LIU W, LIU Q. Annealing behavior of aluminum deformed by equal channel angular pressing [J]. *Mater Lett*, 2003, 57(24/25): 3767–3774.

(Edited by LI Xiang-qun)